Studies on the Sintering Behaviour of UO_2-Gd_2O_3 Fuel Pellets

M. Durazzo[a], H.G. Riella[b]

Abstract. The incorporation of gadolinium directly into nuclear power reactor fuel is important from the point of reactivity compensation and adjustment of power distribution enabling thus longer fuel cycles and optimized fuel utilization. The UO_2-Gd_2O_3 poisoned fuel is being proposed to be implanted in Brazil according to the future requirements established for Angra II nuclear power plant. The incorporation of Gd_2O_3 powder directly into the UO_2 powder by dry mechanical blending is the most attractive process because of its simplicity. Nevertheless, processing by this method leads to difficulties while obtaining sintered pellets with the minimum required density. This is due to blockages during the sintering process. There is little information in published literature about the possible mechanism for this blockage and this is restricted to the hypothesis based on formation of a low diffusivity Gd rich $(U,Gd)O_2$ phase. The objective of this investigation has been to study the blockage mechanism in this system during the sintering process, contributing thus, to clarify the cause for the blockage. Experimentally it has been shown that the blocking mechanism is based on pore formation because of the Kirkendall effect, instead the formation of low diffusivity phases. The formation of a solid solution during the intermediate stage of sintering leads to the formation of large pores, which are difficult to remove in the final stage of sintering. The phenomenon is better characterized as a concurrence between formation and elimination of pores during sintering than as a sintering blockage.

1. Introduction

The need to improve reactor performance through longer cycle lengths or improved fuel utilization has been apparent since the beginning of commercial nuclear power generation. Among several modifications introduced as a consequence, the initial fuel enrichment has been increased, which means that the additional amount of fissile material (^{235}U) in the reactor core has to be compensated by the introduction of additional neutron absorber material in the reactor core. The use of a burnable poison in nuclear reactors provides the necessary negative moderator reactivity coefficient at the beginning of core life and help shape core power distributions [1]. From a nuclear viewpoint, gadolinia is an excellent burnable poison, having a high neutron absorption cross section coupled to a burn up rate that, if properly designed, can match approximately the ^{235}U depletion, minimizing the reactivity penalty at end-of-cycle (EOC) [2,3]. The UO_2-Gd_2O_3 poisoned fuel is being proposed to be implanted in Brazil according to the future requirements established for Angra II nuclear power plant.

From the different methods for the conversion of UF_6 to ceramic grade UO_2 in industrial scale [4], the AUC (Ammonium Uranyl Carbonate) process [5] is the most attractive due to the smallest number of process steps involved. In the AUC process the Gd_2O_3 powder is incorporated to the UO_2 powder by the dry mechanical blending method. Then, the mixed UO_2 and Gd_2O_3 powder is directly pressed into pellet form, without co-milling, pre-pressing and granulating steps [6, 7]. Nevertheless, the incorporation of Gd_2O_3 powder to the AUC deriving UO_2 powder by the most attractive commercial method of dry mechanical blending leads to difficulties while obtaining sintered UO_2-Gd_2O_3 pellets with the minimum required density [7, 8]. This is due to the deleterious effect of the Gd_2O_3 on the traditional UO_2 sintering behaviour. The purpose of this work is to investigate the possible causes for explaining the bad sintering behaviour of the UO_2-Gd_2O_3 fuel prepared by the mechanical blending method.

Several researchers report on the sintering UO_2-Gd_2O_3 mixed oxides, a number of them pointing to difficulties in sintering fuel pellets with the minimal specified density, of around 94% of the theoretical density. Besides, a considerable disagreement between the published data can be observed. Despite the sintering conditions are not identical, the wide variation observed in the final densities of the sintered fuel pellets cannot be explained only based on this reason. The influence of the Gd_2O_3

[a] Nuclear Fuel Centre, Nuclear and Energy Research Institute — IPEN, Brazilian Nuclear Energy Commission — CNEN, São Paulo, Brazil
[b] Chemical Engineering Department, Santa Catarina Federal University, Florianópolis, Brazil

content into the fuel is evident in some sintering results, but it does not appear to be significant in the others. Figure 1 summarizes the final densities achieved by different researchers in sintering UO_2-Gd_2O_3 pellets under reducing atmosphere. A wide range of sintered densities can be observed in this Figure. Table 1 presents the main experimental conditions adopted in the sintering experiments.

The few sintering curves available in the literature show that the lower sintered densities are due to an abnormal sintering behaviour of the UO_2-Gd_2O_3 fuel, when compared with the sintering behaviour of the traditional UO_2 fuel. The dilatometric analyses show that at temperatures around 1100–1400°C, the shrinkage of the UO_2-Gd_2O_3 pellets is delayed, the sintering rate is decreased and the densification is shifted to higher temperatures [7, 17, 18, 20]. Otherwise, sintering curves obtained in previous work [17] showed that the sintering blockage does not occur when the samples are prepared by the coprecipitation method through ADU (Ammonium Diuranate). In this case, very high sintered densities are achieved under the same sintering conditions adopted in the case of dry mechanical blending samples. The gadolinium distribution into the mixed powder is very homogeneous when the coprecipitation method is adopted. This method is mostly used in laboratories to produce homogeneous pellets [9, 21, 22].

As well as the densification results in sintering UO_2-Gd_2O_3 pellets are discrepant and contradictory, likewise are the mechanisms proposed to explain the sintering behaviour. According to Une and Oguma [15], when sintering UO_2-Gd_2O_3 fuel under reducing atmosphere, the system becomes hypostoichiometric to compensate electrically the incorporation of Gd^{3+} ions in the cubic fluorite-type structure of UO_2. Anion vacancies are formed to balance the electrical charge. In this condition, as in the case of the UO_2-PuO_2 system, the cation diffusivity decreases under hypostoichiometric conditions that prevail during sintering, which would explain the low sintered densities achieved while sintering UO_2-Gd_2O_3 fuel pellets. Davis and Potter [19] also attribute the low densities achieved in sintering UO_2-Gd_2O_3 to the hypostoichiometric situation caused by the substitution of U^{4+} ions by Gd^{3+} ions, which would reduce the cation mobility and, consequently, the densification during sintering.

In opposition to the above explanation, Ho and Radford [12] explain their high densities achieved in sintering UO_2-Gd_2O_3 fuel pellets with base in the formation of oxygen vacancies and oxidation of U^{4+} ions. According to these investigators, the electrical charge compensation due to the Gd^{3+} ions incorporation in the UO_2 fluorite structure is accomplished by the formation of oxygen vacancies and oxidation of U^{4+} ions to U^{5+} and/or U^{6+} ions. The oxidation of U^{4+} ions to U^{5+} and U^{6+} ions, which have smaller ionic radii, enhances the cation diffusion and leads to high sintered densities. Above a critical level of Gd_2O_3 addition (around 6 wt%) the diffusivity is inhibited due to the association of Gd^{3+} ions with U^{5+} or U^{6+}. In this case, the associated cations should moves only by cooperative transport, which reduces the sinterability of the system. According to Ho and Radford [12], the increase in the oxygen potential reduces the oxygen vacancies concentration and also allow the creation of oxygen interstitials, which would counterbalance the formation of the small size cations (U^{5+} and U^{6+}), reducing the diffusivity and, therefore, the sinterability. The association of cations also would be favoured.

Manzel and Dörr [7] attribute the low densities observed in sintering UO_2-Gd_2O_3 pellets to the formation of solid solution simultaneously with the densification process. During sintering, the diffusion processes lead not only to the densification but also to the formation of solid solutions. The interdiffusion processes decrease the sintering rate and shift the densification to higher temperatures. Assmann, Pehhs and Roepenack [8] complement this proposition by mentioning that the diffusion coefficients in the UO_2-Gd_2O_3 system depend in a complex manner on the U:Gd:O ratio in the generated oxide phases. Peehs, Dörr, Gradel and Maier [23] detected the presence of the $(U_{0.5}Gd_{0.5})O_2$ phase in sintered UO_2-Gd_2O_3 pellets, without, however, discuss its possible participation in the sintering blockage mechanism. In all these studies, the samples were prepared by the dry mechanical blending method, which used UO_2 powder derived from AUC. Once considered that the sintering blockage occurs during the solid solution formation, that the diffusion coefficient depends on the oxide phases formed and the observation of the $(U_{0.5}Gd_{0.5})O_2$ phase, it can be inferred that the cause proposed for the sintering blockage in the UO_2-Gd_2O_3 system is related to the formation of low diffusivity phases during the sintering process, which reduces the densification and leads to low sintered densities.

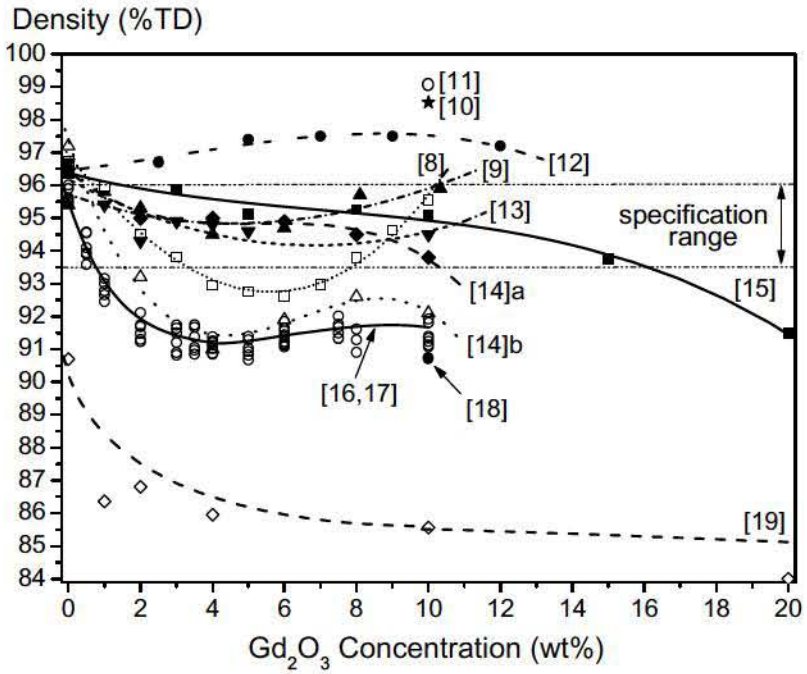

FIG. 1. Effect of gadolinia content on sintered density of UO_2-Gd_2O_3 fuel pellets. TD-theoretical density, specification range from ref. [8].

TABLE 1. MAIN EXPERIMENTAL CONDITIONS FOR THE DATA PRESENTED IN FIGURE 1

Reference	Sintering Cycle (temperature/time) °C/h	UO_2 BET (m^2/g)	Sintering Atmosphere	Method for Mixed Powder Preparation
[9]	1750/4	n.i.	Ar/8%H_2/H_2O	coprecipitation
[10]	1650/4	n.i.	N_2/8%H_2/H_2O	coprecipitation.
[11]	1750/4	n.i.	25%N_2/75%H	co-milling
[12]	1750/6	3.50	H_2/H_2O	co-milling
[13]	1620/3	1.60	pure H_2	co-milling
[14]	1700/2	4.37	pure H_2	co-milling
[14]	1700/2	6.65	pure H_2	co-milling
[8]	1750/2	n.i.	pure H_2	dry blend
[15]	1700/2	3.10	pure H_2	dry blend
[16,17]	1650/3	5.6	pure H_2	dry blend
[18]	1680/4	5.0	pure H_2	dry blend
[19]	1650/4	n.i.	N_2/6%H_2	dry blend

n.i. — not informed.

Yuda and Une [20] proposed that the sinterability of the UO_2-Gd_2O_3 system could not just be evaluated from the viewpoint of cation diffusivity. According to these investigators the two peaks observed in their sintering rate curves correspond to the reaction between adjacent UO_2-UO_2 particles (first peak) and to the reaction between adjacent UO_2-Gd_2O_3 particles (second peak). They proposed the formation of large closed pores due to the difference in the sintering rates between UO_2-UO_2 particles and UO_2-Gd_2O_3 particles. As the large pores are formed in high temperatures, when the pore structure is already partially closed, they are difficult to be eliminated in the posterior sintering treatment. This effect is more intense in oxidizing atmospheres because the pore structure is already essentially closed when the larges pores are formed. This explains the lower density observed in UO_2-Gd_2O_3 pellets sintered under oxidizing atmospheres.

Nishida and Yuda [11] also explain the decrease in the density of samples sintered under higher oxygen potential atmosphere on basis of closed porosities formation. Despite the diffusivity of U and Gd ions is enhanced corresponding with the oxygen potential, under oxidizing atmospheres the effective diffusion length necessary to form solid solution is slightly elongated due to a barrier effect of closed porosities formation, which also results in sintered density decrease.

Song et al. [18] concluded that the sintered density of UO_2-Gd_2O_3 pellets is decreased due to the formation of new pores in the regions with high Gd concentration as the oxygen potential of the sintering atmosphere is increased. The delay of densification occurs together with the solid solution formation in the temperature range of 1300–1500 °C. While the formation of $(U,Gd)O_2$ progresses, new pores are produced at the original sites of Gd_2O_3 particles as a result of the directional diffusion of Gd ions into UO_2. The delay of densification is mainly attributed to the formation of new pores.

The sintering results presented in Figure 1 and the experimental conditions presented in the Table 1 indicate that the method for the UO_2-Gd_2O_3 mixed powder preparation exerts an important influence in the densification during the sintering process. This influence was confirmed by experimental results previously published, presented in Figure 2. The level of homogeneity of the gadolinium distribution in the UO_2 powder determines not only the final sintered density, as well as the form of the sintering curve. When the homogeneity of the gadolinium distribution is good, high densities are obtained during sintering and the sintering blockage is not apparent. On the other hand, when the homogeneity of the gadolinium distribution is bad, low densities are obtained after sintering and the sintering blockage is evidenced, which occurs in two stages [17]. The mechanism proposed by Une and Oguma [15] and Davis and Potter [19] to explain the sintering behaviour of the $UO_2Gd_2O_3$ fuel is not consistent with the results presented in Figure 2. When the gadolinium distribution into the fuel is good, as a solid solution (ADU coprecipitation route), high densities are achieved and no blockage is evidenced. So, the mechanism proposed by Ho and Radford [12] seems to be valid when the gadolinium distribution is homogeneous enough.

On the other hand, when the gadolinium distribution into the fuel is not homogeneous (dry mechanical blending route), the diffusion barrier formation mechanism proposed by Manzel and Dörr [7] (formation of phases with low diffusivity) seems to be possible. Also, the mechanism based on the pore formation during sintering [11, 18, 20] must be considered possible.

In this work, both the mechanisms considered possible are studied. Two hypotheses are proposed and experienced. The first one is based on the formation of low diffusivity $(U,Gd)O_2$ phase that would actuate as a diffusion barrier. The second one is based on the pore formation during sintering. An interesting observation in the UO_2-Gd_2O_3 sintering behaviour is related to the deleterious effect of the oxidizing atmosphere on the densification of UO_2-Gd_2O_3 pellets during sintering. There is a general agreement that the increase in the oxygen potential of the sintering atmosphere causes a significant decrease in the density of the UO_2-Gd_2O_3 pellets after sintering. Another interesting observation is the lower sintered densities observed by Agueda et al. [14] when UO_2 with higher specific surface is used to prepare the mixed powder (dry mechanical blending method). Based on the published data, it can be concluded that the mechanism to be proposed to explain the sintering behaviour of UO_2-Gd_2O_3 fuel pellets must consider the effect of the gadolinium distribution homogeneity into the UO_2-Gd_2O_3 powder, the effect of the oxygen potential of the sintering atmosphere and the effect of the specific surface of the UO_2 powder used to prepare de mixed powder by the dry mechanical blending method.

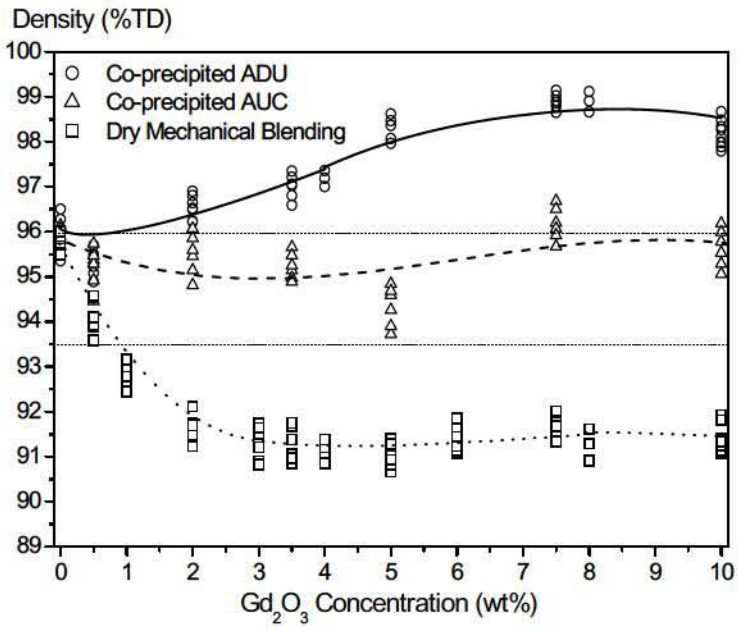

FIG. 2. Effect of the mixed powder preparation method on the sintered density of UO_2-Gd_2O_3 fuel pellets.

2. The diffusion barrier hypothesis

2.1 Phases in the UO_2-Gd_2O_3 system

Once the ADU co-precipitation method for UO_2-Gd_2O_3 powder and pellets preparation demonstrated to result in samples with a high gadolinium homogeneity degree (solid solution) [17], this method was selected for the preparation of samples containing concentrations of Gd_2O_3 from 0 to 100 wt%. These samples made possible the accomplishment of an investigation for verifying the existence of phases with low cation diffusivity in the $(U,Gd)O_2$ system, which could base the diffusion barrier hypothesis. The samples were prepared by coprecipitation from ADU, starting from mixed nitrate solutions, according to procedures previously reported [17].

The variation of the sintered densities as function of the molar fraction of gadolinium present in the sample demonstrates that exist ranges of gadolinium concentration for which the sintered densities are unequivocally decreased, as can be observed in Figure 3. An increase in the sintered density with the increase in the Gd_2O_3 concentration occurs up to 10 wt%, as presented in the Figure 2. This increase reaches a saturation starting from the composition $(U_{0.9}Gd_{0.1})O_2$, when a high densification level is maintained up to the composition $(U_{0.5}Gd_{0.5})O_2$. In this gadolinium concentration range the sintered densities remain in the range varying from 98 to 99% of the theoretical density. These high sintered densities can be explained according to the model proposed by Ho and Radford [12], in which the presence of Gd^{3+} ions causes an increase in the cation diffusivity and, therefore, an increase in the UO_2 sinterability.

When the number of Gd atoms outreaches the number of U atoms (Gd>0.5), the sintered densities decrease drastically and reach a minimum value for the composition $(U_{0.3}Gd_{0.7})O_2$. The further increase in the molar fraction of gadolinium increases the sinterability of the $(U,Gd)O_2$ system again, until reaching a maximum for the composition $(U_{0.2}Gd_{0.8})O_2$, when densities of about 93% of the theoretical density are obtained. After this densification peak, a new decrease in the sinterability is observed. Another minimum is observed in the composition $(U_{0.18}Gd_{0.82})O_2$, when the densification level rises again to reach the typical density for sintering pure Gd_2O_3 pellets (94% of the theoretical density). It is interesting to notice the behaviour of the curve presented in Figure 3 between the compositions $(U_{0.3}Gd_{0.7})O_2$ and $(U_{0.18}Gd_{0.82})O_2$, where it can be observed a peak in the sintered densities. This behaviour was confirmed through repetitions in sintering tests for the composition $(U_{0.2}Gd_{0.8})O_2$ and by sintering the intermediate compositions between Gd=0.7 and Gd=0.9.

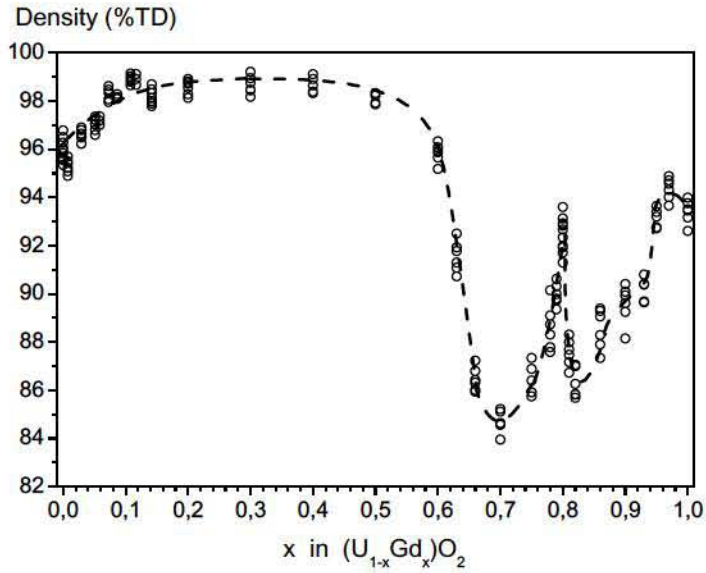

FIG. 3. Effect of the gadolinium concentration on the sintered density of (U,Gd)O_2 pellets prepared by coprecipitation.

The UO_2-Gd_2O_3 sintered pellets were milled and analyzed by X ray diffraction. The lattice parameters of (U,Gd)O_2 were determined with base on the diffractograms by analysing the 2θ position for the more intense (111) planes. Figure 4 presents the variation of the lattice parameter in function of the molar fraction of gadolinium in the sample. A linear decrease on the lattice parameter occurs for compositions up to $(U_{0.5}Gd_{0.5})O_2$, according Vegard's law. This observation indicates the presence of a single phase with fluorite type structure, with Gd^{3+} ions substituting U^{4+} (solid solution). Despite the inaccuracy of this data, a good adjustment for a line can be observed.

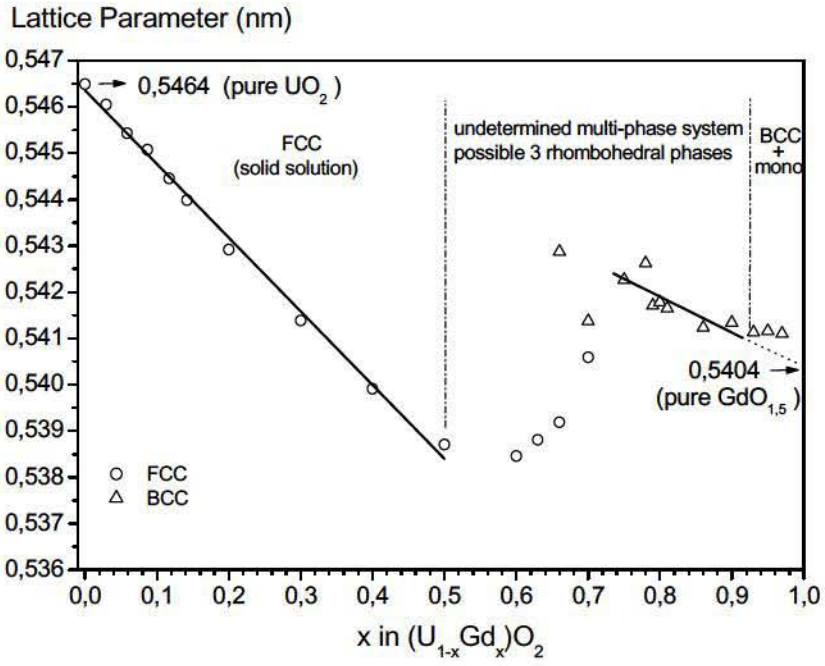

FIG. 4. Variation of the lattice parameter with dissolved gadolinium content.

When the molar fraction of gadolinium outreaches the value 0.5, the behaviour of the lattice parameter of the fluorite structure is not linear anymore, which indicates the end of the single-phase field. For compositions between $(U_{0.25}Gd_{0.75})O_2$ and $(U_{0.10}Gd_{0.90})O_2$, the diffractograms indicate only the presence of the body centered cubic structure, when a tendency to linear decrease on the lattice parameter with the molar fraction of gadolinium can also be observed. However, in this case, it is not possible to affirm that the Vegard's law is obeyed, once a bad adjustment was obtained in a linear regression from the experimental data. This observation may indicate the existence of two or more phases in that composition range. An attempt to fit a straight line to the data is illustrated in Figure 4.

In the intermediate range of composition between $(U_{0.5}Gd_{0.5})O_2$ and $(U_{0.25}Gd_{0.75})O_2$ it cannot be affirmed the simple coexistence between the FCC (face centered cubic) and BCC (body centered cubic) phases, once the lattice parameter is not constant for none of the two structures. For compositions between $(U_{0.25}Gd_{0.75})O_2$ and $(U_{0.1}Gd_{0.9})O_2$ it also cannot be affirmed that the system is single-phase with BCC structure, once cannot be affirmed that the Vegard's law is obeyed. Therefore, in that extensive composition range, where the molar fraction of gadolinium varies from 0.5 to 0.9, the results presented in Figure 4 indicate the existence of one or more phases different from the FCC fluorite structure of UO_2 and BCC structure of Gd_2O_3. For compositions over $(U_{0.10}Gd_{0.90})O_2$ the coexistence between the forms C and B of Gd_2O_3 was evidenced, with structures BCC and monoclinic, respectively.

Aitken, Bartran and Juenke [24] observed a phase with rhombohedral structure in the U-Y-O system, with composition varying in a wide range of yttrium concentration, from 51 to 86 mol%. This phase was designated RI. A second phase was observed in this system, also with rhombohedral structure, designated RII, with composition varying between 68 and 75 mol% yttrium. These two rhombohedral phases were also observed in the U-La-O system and a third rhombohedral phase, designated RIII, was detected in the concentration range varying from 55 to 67 mol% of lanthanum [25]. These rhombohedral phases were also observed in the compounds U-R-O (R=Nd, Sm, Eu, Ho, Er, Tm, Yb and Lu) and in the R-O system, where R=Ce, Pr and Tb, which can present valences +3 and +4. Kang and Eyring [26] observed that these rare earths exhibit a family of binary oxides where coexist the valences +3 and +4, resulting in oxygen deficient fluorite related structures. Among them, the composition R_7O_{12} has the same rhombohedral structure observed in the U-Y-O system. In that and in subsequent reports [27], these researchers propose the construction of crystalline structures of a group of compounds in the R-O system by assembling modules, which are unitary cells of the fluorite structure with oxygen vacancies in different positions in the unitary cell. With base in that mechanism, these researchers established and characterized 14 different phases in the R-O system. The R_7O_{12} phase is isostructural to the rhombohedral UGd_6O_{12} phase.

The experimental observation of the phases built with base in the methodology proposed by Kang and Eyring indicates that an extensive series of phases with structure based on the fluorite structure may exist, where oxygen vacancies are distributed in different ways. This is an important conclusion; once phases that are isostructural to the phases observed by Kang and Eyring in the R-O system may probably also exist in the system U-Gd-O. The U^{4+} cation can be present in these structures substituting the R^{4+} cation. Besides, with the possibility for the existence also of the U^{5+} and U^{6+} cations, the possibility for occurrence of phases more complex than the identified ones cannot be discarded.

Many researchers agree that the stoichiometry in the $(U,Gd)O_2$ system stays close to 2 up to the concentration of 40 mol% Gd_2O_3 [9,28,29,30]. It is also noticed a slight hypostoichiometry for this Gd_2O_3 concentration range. Starting from 40 mol% Gd_2O_3, Beals and Handwerk [28] observed a consistent decrease in the O/M ratio with the increase in the molar fraction of gadolinium, until the value of 1.5 is reached in the case of pure Gd_2O_3. With base in the literature, it can be considered that when Gd^{3+} cations are incorporate in the fluorite structure, U^{4+} cations may be oxidized for charge compensation. According to Ohmich et al [30], the formation of a small proportion of oxygen vacancies may also occurs, probably randomly distributed in the crystal lattice of the solid solution, which is evidenced by the hypostoichiometry. This mechanism, which would be the model 3 proposed by Ho and Radford [12], could be considered valid for Gd_2O_3 concentrations up to 50 mol%.

Above 50 mol% in Gd_2O_3, it is started a systematic formation of oxygen vacancies for charge compensation. When the number of oxygen vacancies reaches a critical value, the oxygen vacancies rearranges to form new phases that would be isostructural to the ones observed and modelled by Kang and Eyring in the R-O system, as discussed previously. The rhombohedral phase would probably be one of them. In that way, the variation on the lattice parameter as function of the molar fraction of gadolinium stops satisfying the Vegard's law. With the continuous increase in the number of oxygen vacancies, the crystalline structure develops until obtaining the BCC structure of Gd_2O_3, where 16 oxygen vacancies are present. If the straight line that represents the variation of the lattice parameter in the composition range of x = 0.75 to 0.9 is extrapolated, it intercepts the ordinate axis at the value 0.5404 nm for x = 1 ($GdO_{1.5}$), which is very close to the X ray diffraction standard value of 1.0813 nm for the Gd_2O_3 unitary cell, or 0.5407 nm for the pseudo fluorite cell of the $GdO_{1.5}$.

The beginning in the sinterability decrease in the UO_2-Gd_2O_3 system corresponds to the end of the monophase area in the system, with fluorite structure, for the composition $(U_{0.5}Gd_{0.5})O_2$ (see Figures 3 and 4). This also corresponds to the beginning of the systematic formation of oxygen vacancies, evidenced by the decrease in the O/M ratio, which was almost constant until approximately this composition, according to the literature [28]. Although the new $(U,Gd)O_2$ phases have not been observed directly in this work, the results of this work support the proposition that the beginning of the systematic oxygen vacancies formation makes possible the formation of new $(U,Gd)O_2$ phases in the system, which are different from the fluorite phase. One probable phase is the rhombohedral phase observed in the U-Y-O system, which should be isostructural to the one observed in the rare earth oxides CeO_{2-x}, PrO_{2-x} and TbO_{2-x}. This complex phase structure would be responsible for the decrease in the cation diffusivity of the system, leading to the decrease in the sinterability. The presence of some phase with good diffusivity (not detected directly in this work) could be responsible for the form of the curve presented in Figure 3, which revealed good sinterability for the composition $(U_{0.2}Gd_{0.8})O_2$.

The experimental results presented in the Figure 3 give base for the proposed Diffusion Barrier Hypothesis, once molar fractions of gadolinium higher than 0.5 results in very low sintered densities. The occurrence of phases different from fluorite for molar fractions of gadolinium higher than 0.5 was also observed, what could explain the decrease in the sinterability. However, nothing can be affirmed about the dependence of the interdiffusion coefficient in the UO_2-Gd_2O_3 system on the gadolinium concentration, which ultimately is what determines the sinterability of the system. Aiming at giving additional support for the proposed hypothesis, an interdiffusion study in the system UO_2-Gd_2O_3 was accomplished, whose results are presented and discussed in the next item.

2.2 Interdiffusion studies

The interdiffusion studies were accomplished by determining the gadolinium concentration profile (penetration curves) in a couple of sintered UO_2/Gd_2O_3. The interdiffusion coefficient was determined in function of the molar fraction of gadolinium by applying the Matano-Boltzman method [31]. The UO_2/Gd_2O_3 couple was prepared by compacting simultaneously both the UO_2 and Gd_2O_3 powders. The couple was sintered at 1650 °C for 3 hours. The couple obtained after sintering presented good mechanical resistance in the interface, which makes possible its longitudinal cut, perpendicular to the interface. The surface of the sample was prepared through conventional metallographic techniques.

Initially, a qualitative analysis was accomplished in the polished surface, where the appearance of the UO_2/Gd_2O_3 interface was revealed through scanning electron microscopy. The general form of the concentration profile was determined through qualitative analysis (EDS - Energy-dispersive X ray spectroscopy) of the gadolinium concentration over a line perpendicular to the interface. In three areas, it was accomplished a quantitative analyses for the gadolinium concentration through WDS (Wavelength dispersive X ray spectroscopy) in points spaced by 0.5 µm. The precision in the determination of the gadolinium concentration was esteemed to be 0.1%. From the penetration curves, the interdiffusion coefficient was determined through graphic integration applying the Matano-Boltzmann method. Figure 5 presents an electronic micrograph illustrating the UO_2/Gd_2O_3 interface. In general, it was observed the presence of a void between the phases, with width between 1 and 3 µm. The uranium and gadolinium concentrations were determined along the line indicated in the Figure.

The concentration profiles indicate interpenetration of approximately 16 µm after sintering for 3 hours at 1650 °C. The gadolinium penetration into the UO_2 phase is sensibly higher than the uranium penetration into Gd_2O_3 phase (higher than 2/3 of the total interpenetration distance).

An inspection was accomplished along the interface with aiming at selecting areas with good continuity between the UO_2 and Gd_2O_3 phases, where the width of the void was minimal. Three areas were selected, which presented a good continuity between the phases. In those areas quantitative analyses were performed for gadolinium concentration determination in points spaced 0.5 µm along a line normal to the UO_2/Gd_2O_3 interface line. The experimental points are presented in Figure 6. Once constructed the penetration curve, the interdiffusion coefficient in the UO_2-Gd_2O_3 system was calculated in function of the molar fraction of gadolinium by applying the data analysis method proposed by Matano [31].

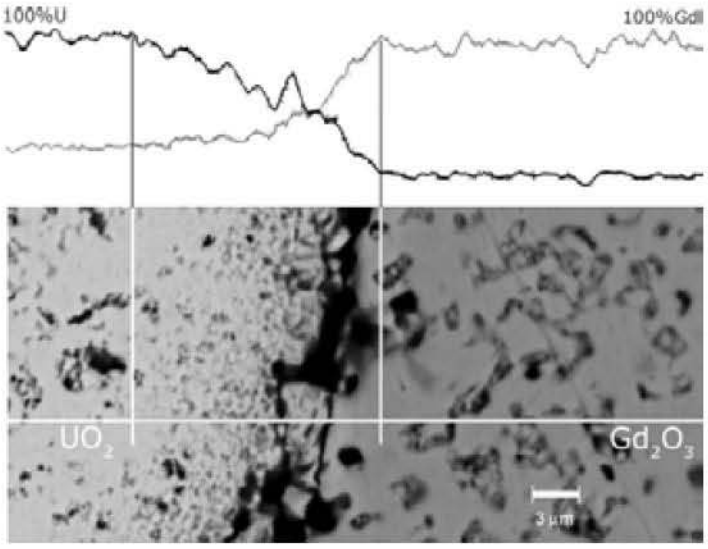

FIG. 5. Scanning electron micrograph illustrating the UO_2/Gd_2O_3 interface.

The interdiffusion coefficient was calculated for 0 to 100 mol% of gadolinium. The results are presented in Figure 7. The most important characteristic in this Figure is the sudden decrease in the interdiffusion coefficient for gadolinium concentrations above 50 mol%. It is also interesting to observe the increase in the interdiffusion coefficient value for gadolinium concentrations of about 80 mol%. These results are in good agreement with the results presented in Figure 3, and confirm in a direct way that the interdiffusion coefficient in the UO_2-Gd_2O_3 system decreases abruptly when the molar fraction of gadolinium is higher than 0.5, or when more than half of the cations presents are Gd^{3+}. Despite the imprecision of the applied method, which is evidenced by the considerable dispersion in the experimental data presented in Figure 7, it is conclusive that the UO_2-Gd_2O_3 sinterability decreases drastically starting from the composition $(U_{0.5}Gd_{0.5})O_2$ due to a sudden decrease in the interdiffusion coefficient of the system starting from that composition.

The presented results give base for the Barrier Diffusion Hypothesis. The sinterability of the system is drastically decreased for concentrations higher than 50 mol% Gd_2O_3, as is unequivocally shown in Figure 3. The cause for the sinterability decrease seems to be the sudden decrease on the interdiffusion coefficient for concentrations higher than 50 mol% Gd_2O_3, as is shown in Figure 7. Although they have not been detected directly, other unidentified phases with crystalline structure different from the fluorite probably exist for concentrations higher than 50 mol% Gd_2O_3, as is indicated by the variation of the lattice parameter presented in Figure 4. This observation is reinforced by the identification of a series of phases in the systems (Ce, Pr, Tb)-O, which probably have the same crystalline structure of the phases still not identified in the system U-Gd-O, once the model for construction of these phases in the rare earth oxides is entirely applicable for the UO_2-Gd_2O_3 system.

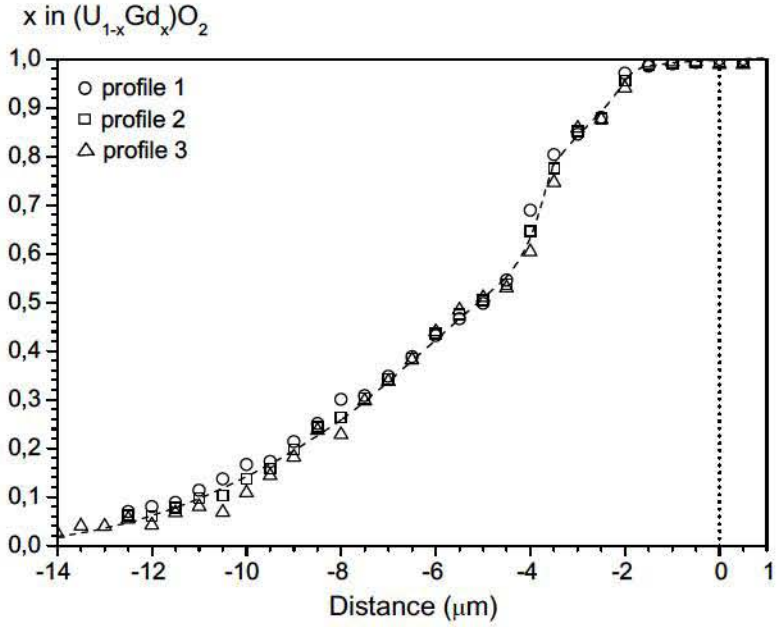

FIG. 6. Concentration profile across the UO_2/Gd_2O_3 interface.

2.3 Testing the hypothesis

The methodology adopted for testing the hypothesis is based on performing a sintering test in mixed powders where the Gd_2O_3 is incorporated to the UO_2 in such a way that guarantees the diffusion barrier is not formed. In other words, it is guaranteed that the Gd_2O_3 concentration never surpasses the value of 50 mol%. As the formation of low sinterability phases different from the fluorite just begins for Gd_2O_3 concentrations higher than 50 mol%, as previously discussed, mixed powders were prepared where the pure Gd_2O_3 powder was substituted by powders prepared by coprecipitation containing Gd_2O_3 concentrations inferior to 50 mol%. In that case, the formation of phases with gadolinium concentration above 50 mol% is not possible during the gadolinium solubilization, and the formation of the diffusion barrier also is not possible. According to the results presented in Figure 3, this new mixed powder presents sinterability higher than pure UO_2, once the presence of gadolinium in the fluorite structure favors the sintering process.

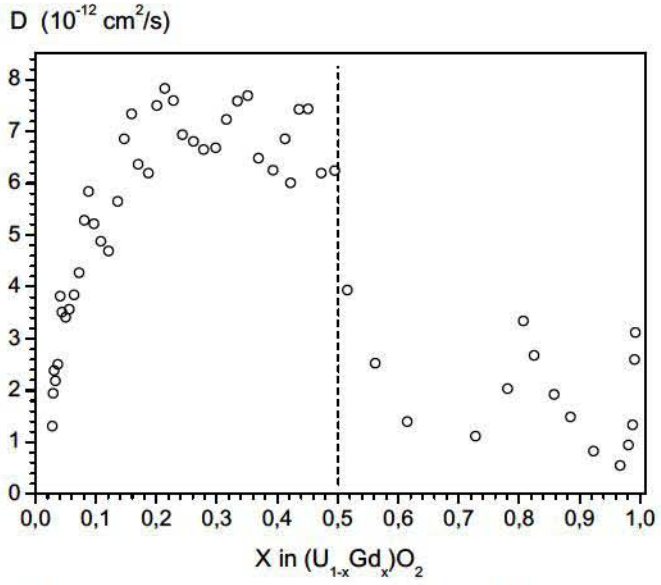

FIG. 7. Interdiffusion coefficient as function of the molar fraction of gadolinium.

Powders obtained by coprecipitation via ADU, which presents good homogeneity, were mechanically blended with UO_2 powder by homogenizing the mixture in a shaker mixer. Powders prepared by coprecipitation with compositions of 20, 30, 40, 50, 60, 70, 80 and 90 mol% of Gd_2O_3 were added to the UO_2 powder in order to always obtain the equivalent concentration of 10 wt% Gd_2O_3 (or 14,2 mol%) in the sample. The samples were compacted and sintered under the same conditions used previously (1650 °C for 3 hours under H_2 atmosphere). After sintering, the densities were determined by measuring the weight of samples immersed in xylol (Archimedes principle). The results are presented in Figure 8.

As previously mentioned, the sinterability decrease in the UO_2-Gd_2O_3 system, or the interdiffusion coefficient decrease, is probably due to the formation of phases different from the fluorite structure of UO_2 and it only happens for Gd_2O_3 concentrations above 50 mol%. Below that concentration the only one phase present is a solid solution where Gd^{3+} cations substitute U^{4+} cations in the fluorite structure, which is beneficial in terms of sinterability of the system, as it is illustrated in Figure 3. Therefore, the formation of the diffusion barrier is unable to happen when pure Gd_2O_3 powder is substituted by coprecipitated powders containing Gd_2O_3 concentrations smaller than 50 mol% in preparing the mixed oxides by mechanical blending. In this case, it becomes impossible the occurrence of areas where the gadolinium concentration exceeds 50 mol% in mol and, therefore, it becomes impossible the formation of low diffusivity phases that could act as a diffusion barrier. In that condition, the presence of gadolinium should necessarily increase the sinterability of the system, even when it is added through the mechanical blending method. The sintered density expected would be the one observed in sintering coprecipitated powder containing 10 wt% Gd_2O_3 (or 14,2 mol%). With base in the diffusion barrier hypothesis, the minimum acceptable sintered density would be the one correspondent to pure UO_2 (indicated in Figure 8), supposing that the presence of gadolinium does not affect the UO_2 sinterability. The results presented in Figure 8 show a behavior that does not support the diffusion barrier hypothesis.

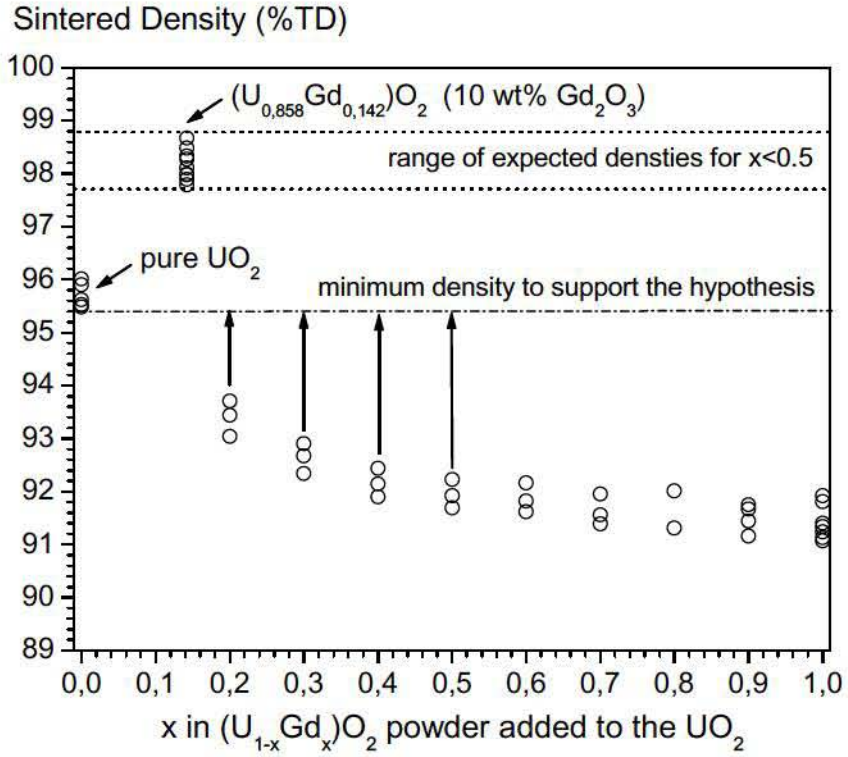

FIG. 8. Densification levels observed in sintering UO_2-Gd_2O_3 pellets prepared by mechanical blending using $(U_{1-x}Gd_x)O_2$ coprecipitated mixed powders.

If the nominal Gd_2O_3 concentration in all the sintered pellets is 10 wt% (or 14,2 mol%), it is not possible the formation of areas where the Gd_2O_3 concentration is superior to 50 mol% during sintering samples which are prepared with coprecipitated mixed powders with composition inferior to $(U_{0.5}Gd_{0.5})O_2$. As the interdiffusion coefficients stay in a constant level between the molar fractions of gadolinium varying from 0.2 to 0.5 (see Figure 7), in the range from 6 to $8x10^{-16}$ m^2/s, the final density expected after sintering mechanically blended mixed powders prepared with coprecipitated powders with compositions of gadolinium inferior to 50 mol% should necessarily be compatible with the density level observed in sintering pellets containing 10 wt% Gd_2O_3 prepared by coprecipitation (approximately 98%TD). Even so adopting an extreme hypothesis, which would consider that does not happen any gadolinium redistribution during sintering, the minimum acceptable density that would support the Diffusion Barrier Hypothesis would be the typical density obtained in sintering pure UO_2 (approximately 95.5%TD), which did not also happen. The experimental evidence that would support the hypothesis would be an abrupt increase in the sintered density obtained in the samples prepared with mixtures UO_2- $(U_{1-x}Gd_x)O_2$, with $X \leq 0.5$. Low densities should be observed only for values of X superior to 0.5 in the formula, once, in that case, the formation of low diffusivity phases is possible.

Consequently, with base in the experimental results obtained in testing the hypothesis, the formation of a diffusion barrier to explain the sintering behavior of UO_2-Gd_2O_3 fuel pellets must be rejected as a possible mechanism.

3. The pore formation hypothesis

An interesting observation on the results obtained in the interdiffusion studies presented previously is related to the shape of the penetration curve presented in Figures 5 and 6. The results indicate that the material flow is not homogeneous, with Gd^{3+} cations penetrating preferentially in the UO_2 fluorite structure. In Figure 5 is evident the largest penetration of the gadolinium in the UO_2 phase when the position of the interface UO_2/Gd_2O_3 is taken as reference. Those observations indicated that the Kirkendall effect seems to be occurring in this system.

The diffusion between the components of the mixture during sintering the UO_2-Gd_2O_3 fuel prepared by the mechanical blending method happens simultaneously. If the diffusion rate of the two species of atoms is not the same, the Kirkendall effect occurs. In other words, if the gadolinium cations diffuse more quickly into the UO_2 phase than the opposite, a larger flow of gadolinium deriving from the Gd_2O_3 agglomerates in direction to the UO_2 phase is established, when compared with the uranium flow in direction to the interior of the Gd_2O_3 agglomerates. In this case, the UO_2 phase expands for receiving the extra gadolinium cations and a void is generated at the place of the original Gd_2O_3 agglomerate. This phenomenon is commonly observed in mixed powders systems where exists an unbalanced diffusivity or solubility between the powders [32].

As the pore formation due to this effect occurs at temperatures in which the pore structure is essentially closed, during the second stage of sintering, the pore elimination is probably very difficult. The possibility of occurrence of this phenomenon in the UO_2-Gd_2O_3 system gives base for the Pore Formation Hypothesis.

3.1 Experimental evidences

The results obtained in the interdiffusion studies revealed that the penetration of the gadolinium into the UO_2 is considerably larger than the penetration of the uranium into the Gd_2O_3 (see Figure 5).

Although the individual diffusion coefficients was not determined in this work and the individual diffusion coefficients of gadolinium into the UO_2 and uranium into Gd_2O_3 have not been found in the literature, it is known that uranium diffuses very little in the cubic form of Gd_2O_3 and the diffusion of uranium in the B form of Gd_2O_3 (monoclinic) is practically null. In the UO_2-Y_2O_3 system the maximum solubility of uranium in the cubic Y_2O_3 (C form) is 7–8 mol% [33]. The maximum solubility of uranium in the B form Gd_2O_3 is 2 mol% [34, 35]. In conclusion, all the information indicates low solubility of uranium in both cubic and monoclinic forms of Gd_2O_3. On the contrary,

gadolinium diffuses easily into the UO_2 fluorite structure, as is illustrated in Figure 4, which shows a wide range of gadolinium concentration where solid solution is formed.

Therefore, the experimental results obtained in this work and the information obtained in the literature indicate that a considerable difference exists between the diffusion coefficients of gadolinium into UO_2 and uranium into Gd_2O_3 (both forms C and B), which could cause an unbalancing in material transport during the solid solution formation when sintering the UO_2-Gd_2O_3 fuel prepared by the mechanical blending method, where Gd_2O_3 agglomerates are dispersed in a UO_2 matrix before sintering. In this situation is probable the occurrence of the Kirkendall effect.

The morphology of the Gd_2O_3 powder and the pore structure developed in sintered UO_2-Gd_2O_3 pellets prepared by the mechanical blending method supports the pore formation hypothesis. The morphology of the Gd_2O_3 powder is illustrated in Figure 9. The presence of Gd_2O_3 agglomerates with large diameter (>40 μm) is evidenced. In sintered UO_2-Gd_2O_3 pellets prepared by mechanical blending, it is observed the existence of pores with diameters sensibly larger than the pore diameter typically observed in pure UO_2 sintered pellets. The curve of pore diameter distribution is shifted in the direction of larger diameters. This effect is illustrated in Figure 10. In this Figure it is observed that the pore diameter distribution in the pure UO_2 fuel pellet agrees well with the pore diameter distribution typical for the UO_2 fuel fabricated starting from TCAU, which varies between 0.5 μm and about 10 μm with average between 3 and 4 μm [6,36]. In the case of the sample containing 10 wt% Gd_2O_3, it is observed pores with diameter up to 25 μm, with the average moved to approximately 8 μm. This resulted supports the proposition of the hypothesis, once the Gd_2O_3 agglomerates existent in the system (see Figure 9) can result in the formation of pores due to the Kirkendall effect occurrence during the solid solution formation, simultaneously with the sintering process. That pores could not be eliminated (at least not totally) during the sintering stage subsequent to their formation.

With base in these observations, which already bases the hypothesis by itself, is possible to propose that during the sintering of the UO_2-Gd_2O_3 fuel prepared by the mechanical blending method occurs simultaneously the formation of the $(U,Gd)O_2$ solid solution. The formation of large pores due to the Kirkendall effect happens during the formation of the solid solution, in places where originally existed Gd_2O_3 agglomerates, due to the preferential solubilization of gadolinium into the fluorite structure of UO_2, These large pores, once formed in high temperature, are difficult to be eliminated in the subsequent sintering stages and remain in the sintered pellet in the form of stable pores, which causes the decrease of the final sintered density. The formation of stable pores during sintering (Kirkendall effect) would be responsible for the sintering behavior of the UO_2-Gd_2O_3 fuel prepared according to the mechanical blending method due to the presence of Gd_2O_3 agglomerates in the green pellets.

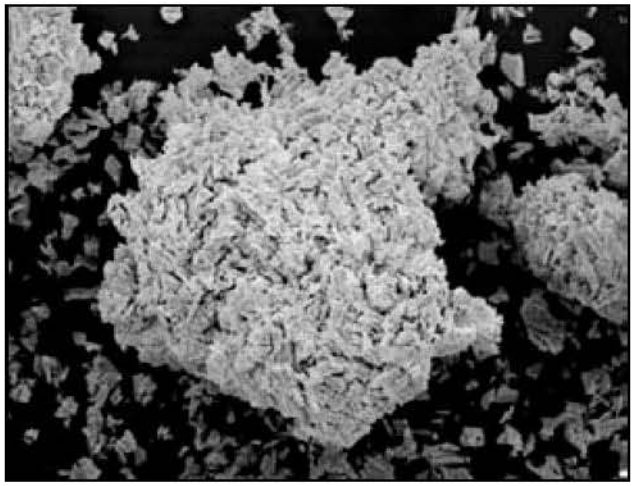

FIG. 9. Scanning electron micrography illustrating Gd_2O_3 agglomerate.

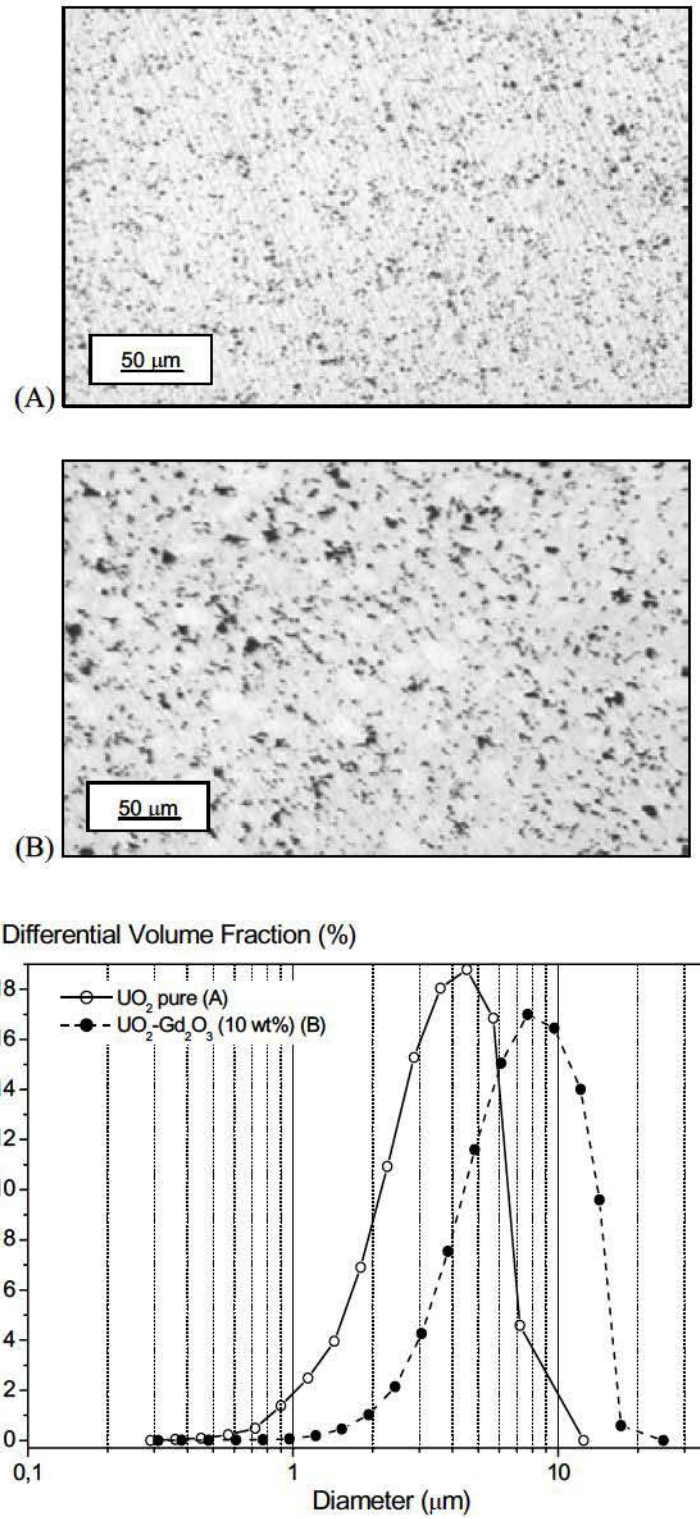

FIG. 10. Optical micrographies and pore diameter distribution curves for:A) pure UO_2 and B) UO_2-Gd_2O_3 (10 wt% Gd_2O_3)

3.2 Testing the hypothesis

The hypothesis test was accomplished through the preparation of UO_2-Gd_2O_3 pellets where Gd_2O_3 agglomerates of controlled size were added to the UO_2 powder by the mechanical blending method. The Gd_2O_3 agglomerates were obtained by compacting and granulating the original Gd_2O_3 powder. The granules were classified in the size ranges <37 µm, between 37 and 45 µm, between 45 and 53

μm and between 53 and 62 μm. The Gd_2O_3 concentration was 10 wt%. The UO_2-Gd_2O_3 mixtures prepared with Gd_2O_3 granules of different size were compacted and sintered at 1650 °C for 3 hours under H_2 atmosphere. Polished sections of the sintered pellets were observed in optical microscope and the pore diameter distributions were determined.

The micrographies presented in Figure 11 show pore structures with pore diameters superior to the range of diameters typically observed in the standard UO_2 fuel fabricated starting from AUC, which varies between 0.5 μm and about 10 μm [6,36]. In those micrographies it is possible to observe a consistent increase in the diameter of the big pores with the increase in the diameter of the Gd_2O_3 granules mixed to the UO_2 powder. In the micrographies corresponding to Gd_2O_3 granules superior to 45 μm, it is possible to observe that some granules were not totally solubilized in the UO_2 fluorite structure. A growing void around the granule perimeter can be observed. This experimental observation demonstrates that the big pores observed in the micrographies of Figure 11 were really formed at places where initially existed Gd_2O_3 granules. Those pores are responsible for the bimodal form of the pore diameter distributions presented in Figure 11. Unlike the typical monomodal distribution, which is characteristic of the standard UO_2 fuel prepared starting from AUC, it is observed that all the pore diameter distributions obtained are bimodal. It is also observed that the position of the second peak of the distributions is related to the granulometry of the added Gd_2O_3 granules. As larger are the Gd_2O_3 granules present, larger are the pore diameter corresponding to the second peak of the bimodal distribution. If the size of the Gd_2O_3 agglomerate is sufficiently small, the diameter of the pore formed due to the Kirkendall effect is incorporated in the first peak of the bimodal distribution, which results in a monomodal distribution shifted in the direction of larger diameters (see Figure 10B). The scanning electron micrograph presented in Figure 12 illustrates the formation of pores due to the Kirkendall effect. Part of the gadolinium of the Gd_2O_3 agglomerate was already diffused into the UO_2 matrix, but the solubilization is not complete. This Figure shows Gd_2O_3 agglomerate inside a pore in formation.

The correlation between the pore diameter in the second peak of the bimodal distribution and the presence of Gd_2O_3 inside pores in formation demonstrate that those pores of larger diameter are generated starting from Gd_2O_3 agglomerates by occasion of their dissolution in the crystal lattice of UO_2 during sintering, which is resulted from the Kirkendall effect occurrence. As the formation of solid solution occurs at elevated temperatures when the pore structure is probably already essentially closed, during the second stage of sintering, the pores formed cannot be eliminated, at least not entirely, resulting in a sintered body with larger residual porosity.

The mechanism based on the formation of stable pores during sintering explains the strong influence that the homogeneity of the Gd_2O_3 powder distribution in the UO_2-Gd_2O_3 mixed powder exerts on the density obtained after sintering [17]. This mechanism also explains the lowering in the sintered densities with the increase in the oxygen potential of the sintering atmosphere. In this case, as the sintering process is favored and proceeds at lower temperatures, the pore formation due the Kirkendall effect occurs in a much closed pore structure, which essentially impedes their elimination because the sintering process is almost totally finished when the pores are formed.

The pore formation mechanism also explains the influence of the specific surface of the UO_2 powder on the sintered densities of UO_2-Gd_2O_3 pellets, as pointed by the results obtained by Agueda et al. [14] (see Figure 1 and Table 1). If the specific surface of the UO_2 powder is high, the sintering process is favored and the pore structure closes at lower temperatures, which makes difficult the elimination of the pores formed due the Kirkendall effect. On the other hand, if the specific surface of the UO_2 powder is low enough, the sintering process is sufficiently delayed in order to allow the formation of pores due the Kirkendall effect in a pore structure open enough to help their further elimination. In other words, if the specific surface of the UO_2 powder is adequate, a reserve of activity for sintering in higher temperatures would be available in order to close the pores formed due the Kirkendall effect.

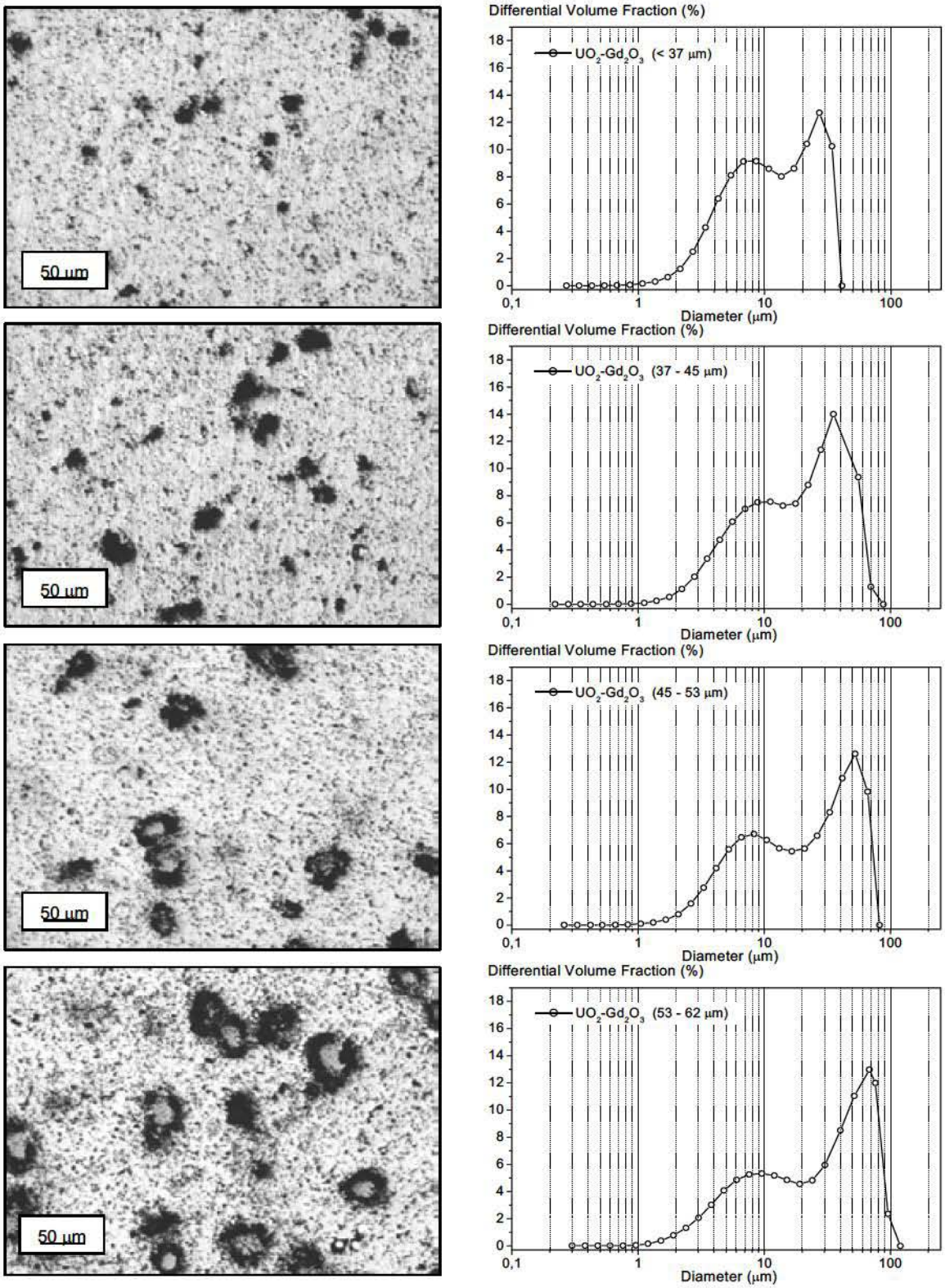

FIG. 11. Pore structure of sintered UO_2-Gd_2O_3 pellets prepared with Gd_2O_3 granules of different sizes.

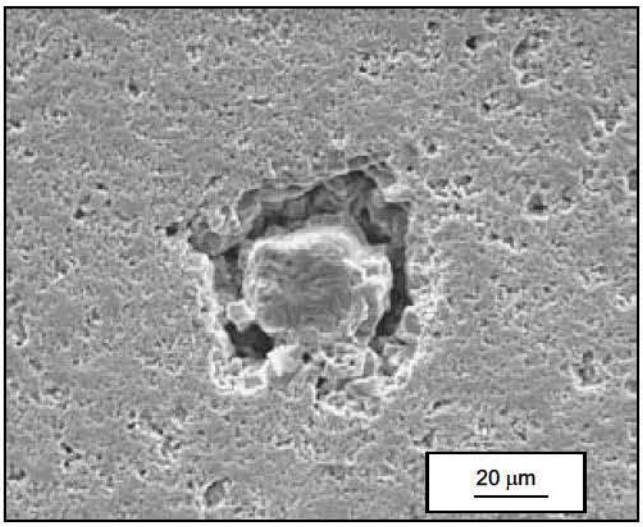

FIG. 12. Scanning electron micrography illustrating the pore formation at Gd_2O_3 agglomerate original places.

4. Conclusions

With base in the obtained experimental evidences, the hypothesis based on the formation of stable pores can be considered demonstrated. Although phases different from the fluorite were indirectly detected, which have low cation diffusivity; the hypothesis based on the formation of a diffusion barrier must be rejected. The phenomenon is better characterized as a concurrence between pore formation and elimination during sintering than as a sintering blockage.

The mechanism that explains the sintering behavior of the UO_2-Gd_2O_3 fuel prepared by the mechanical blending method and using UO_2 powder derived from the AUC technology is based on the occurrence of the Kirkendall effect. A significant difference in the interdiffusion coefficients of the gadolinium into UO_2 and of the uranium into Gd_2O_3 causes a misbalancing in the material transport during the solid solution formation. As consequence of this phenomenon, the densification during sintering occurs simultaneously with the formation of pores in places where originally Gd_2O_3 agglomerates were present. The diameters of these pores are proportional to the initial diameter of the agglomerates present and they are stable, once they have been formed in high temperature in an essentially closed pore structure. Under this situation, it is not possible the elimination of that pores after their formation, in the subsequent sintering process. That pores remain in the sintered pellet and causes the low densities observed.

ACKNOWLEDGEMENTS

The authors wish to express their gratitude to CTMSP (Navy Technological Center in São Paulo) for the permission to use its facilities. The authors also wish to express their sincere thanks to the staffs of the Nuclear Materials Laboratory of CTMSP for their helps in the course of this study.

REFERENCES

[1] BÖHM, W., KIEHLMANN, H.D., NEUFERT, A., PEEHS, M., Gd_2O_3 up to 9 weight percent, an established burnable poison for advanced furl management in pressurized water reactors, Kerntechnik **50,** (1987), p.234.

[2] HELLSTRAND, E., Burnable poison reactivity control and other techniques to increase fuel burnup in LWR fuel cycles, Trans. Am. Nucl. Soc. **40,** (1982), p.181.

[3] SKOGEN, F.B., NIELSEN, L.A., GRUMMER, R.G., Operation experience with Exxon nuclear-supplied Gadolinia in Pressurized Water Reactors, Trans. Am. Nucl. Soc. **40,** (1982), p.194.

[4] BRANDBERG, S.G., The conversion of uranium hexafluoride to uranium dioxide, Nuclear Technology **18,** (1973), p.177.

[5] ASSMANN, H., BECKER, M., Technology of UO_2 fuel fabrication by the AUC powder process, Trans. Am. Nucl. Soc. **31,** (1979), p.147.

[6] ASSMANN, H., DÖRR, W., Microstructure and density of UO_2 pellets for Light Water Reactors as Related to Powder Properties, Materials Science Monographs **16,** (1983), 707.

[7] MANZEL, R., DÖRR, W., Manufacturing and irradiation experience with UO_2/Gd_2O_3 fuel, Am. Ceram. Soc. Bull. **59,** 6, (1980), p.601.

[8] ASSMANN, H., PEEHS, M., ROEPENACK, H., Survey of binary oxide fuel manufacturing and quality vontrol, J. Nucl. Mater. **153,** (1988), p.115.

[9] FUKUSHIMA, S., OHMICHI, T., MAEDA, A., WATANABE, H., The effect of Gadolinium content on the thermal conductivity of near-stoichiometric $(U,Gd)O_2$ solid solutions, J. Nucl. Mater. **105,** (1982), p. 201.

[10] HIRAI, M., Thermal diffusivity of UO_2-Gd_2O_3 pellets, J. Nucl. Mater. **173,** (1990), p.247.

[11] NISHIDA, T., YUDA, R., Effect of particle size and oxygen potential on UO_2/Gd_2O_3 pellet sintering, Advances in Fuel Pellet Technology for Improved Performance at High Burnup, IAEA–TECDOC—**1036**, Vienna, (1998), p.73.

[12] HO, S.M., RADFORD, K.C., Structural chemistry of solid solutions in the UO_2-Gd_2O_3 system, Nuclear Technology **73,** (1973), p.350.

[13] LITTLECHILD, J.E., BUTTLER, G.G., LESTER, G.W., The production of burnable poison oxide fuel, Nuclear Fuel Performance 1973, Proc. Int. Conf. London, Vol. **1**, London, (1973), p. 65.

[14] AGUEDA, H.C., HEREDIA, A.D., AMAYA, D.C., STERBA, M. E., RUSSO, D., Efectos del oxido de Gadolínio en la sinterization de dioxido de uranio", General Congress on Nuclear Energy, Proc. Conf. Rio de Janeiro, Vol. **2**, Rio de Janeiro, (1994), p.567.

[15] UNE, K., OGUMA, M., Oxygen potential of $U_{0.96}Gd_{0.04}O_2$ (UO_2-3wt% Gd_2O_3) solid solution, J. Nucl. Mater. **131,** (1985), p.88.

[16] RIELLA, H.G., DURRAZO, M., HIRATA, M., NOGUEIRA, R.A., UO_2-Gd_2O_3 solid solution formation from wet and dry processes, J. Nucl. Mater. **178,** (1991), p.204.

[17] DURAZZO, M., RIELLA, H.G., Effect of mixed powder homogeneity on the UO_2-Gd_2O_3 nuclear fuel sintering behavior, Key Eng. Mat. **189–191,** (2001), p.60.

[18] SONG, K.W., KIM, K.S., YANG, J.H., KANG, K.W, JUNG, Y.H., A mechanism for the sintered density decrease of UO_2-Gd_2O_3 pellets under an oxidizing atmosphere, J. Nucl. Mater. **288,** (2001), p.92.

[19] DAVIS, H.H., POTTER, R.A., UO_2-Gd_2O_3 sintering behavior, Materials Science Research **11,** (1977), p.515.

[20] YUDA, R., UNE, K., Effect of sintering atmosphere on the densification of UO_2-Gd_2O_3 compacts, J. Nucl. Mater. **178,** (1991), p.195.

[21] WADA, T., NORO, K., TSUKUI, K., Behavior of UO_2-Gd_2O_3 fuel, Nuclear Fuel Performance, Proc. Int. Conf. London, (1973), p.63.

[22] MIYAKE, C., KANAMARU, M., IMOTO, S., Microcharacterization of Gadolinium in $U_{1-x}Gd_xO_2$ by means of electron spin resonance, J. Nucl. Mater. **137,** (1986), p.256.

[23] PEEHS, M., DÖRR, W., GRADEL, G., MAIER, G., Zur Wärmleitfähigkeit und Plastizität von UO_2 mit Gd-Zusätzen, J. Nucl. Mater. **106,** (1982), p.221.

[24] AITKEN, E.A., BARTRAM, S.F., JUENKE, E.F., Crystal chemistry of the rombohedral $MO_3.3R_2O_3$ compounds, Inorg. Chem. **3,** (1964), p.959.
[25] GSCHNEIDER Jr, K.A., EYRING, L. Handbook on the physics and chemistry of rare earths. Non-Metallic compounds-I, Vol. **3**, North-Holand Physics Publishing, Amsterdam (1979), p.444.
[26] KANG, Z.C., EYRING, L., A Compositional and structural rationalization of the higher oxides of Ce, Pr, and Tb, Journal of Alloys and Compounds **249,** (1997), p.206.
[27] KANG, Z.C., EYRING, L., The prediction of the structure of members of the homologous series of the higher rare earth oxides, Journal of Alloys and Compounds **275–277,** (1998) p.30.
[28] BEALS, R.J., HANDWERK, J.H., Solid solutions in the system urania-rare-earth oxides, J.Am. Ceram. Soc. **48,** (1965), p.271.
[29] UNE, K., OGUMA, M., Thermodynamic properties of nonstoichiometric urania Gadolinia solid solutions in the temperature range 700–1100 °C, J. Nucl. Mat. **110,** (1982), p.215.
[30] OHMICHI, T., FUKUSHIMA, S., MAEDA, A., WATANABE, H., On the relation between lattice parameter and o/m ratio for uranium dioxide–trivalent rare earth oxides: I, UO_2-$GdO_{1.5}$, J. Nucl. Mat. **102** (1981) 40.
[31] MATANO, C., On the relation between diffusion-coefficients and concentration of solid metals (the nickel-copper system), Japanese Journal of Physics **8,** (1933), p.109.
[32] GERMAN, R.M., Sintering theory and practice, John Willey and Sons, New York, (1996).
[33] GSCHNEIDER Jr, K.A., EYRING, L., Handbook on the physics and chemistry of rare earths. Non-Metallic Compounds–I, Vol. **3**, North-Holand Physics Publishing, Amsterdan (1979), p.444.
[34] BEALS, R.J., HANDWERK, J.H., WRONA, B.J., Behavior of urania-rare-earth oxides at high temperatures, J.Am. Ceram. Soc. **52,** 11, (1969), p.578.
[35] KELLER, C., Ternäre und polynäre Oxide des Urans, Gmelin Handbuch der Anorganischen Chemie, Springer-Verlag, Berlin, (1975).
[36] ASSMANN, H., DÖRR, W., PEEHS, M., Oxide fuels with controlled microstructure, J. Am. Ceram. Soc. **67,** (1984), p.631.